IFIC ATLASVLC
Instituto de Física Corpuscular - Valencia

Constraints on effective field theories via quadruple-differential angular decay rates from single-top-quark at ATLAS

arXiv:2510.23372

Mariam Chitishvili

Instituto de Fisica Corpuscular (IFIC), Centro Mixto
Universidad de Valencia - CSIC, Valencia, Spain

CSIC Consejo Superior de Investigaciones Científicas
Universitat de València
IFIC Institut de Física Corpuscular
Generalitat Valenciana CIPROM/2022/70
Ministerio de Ciencia, Innovación y Universidades
Unión Europea Fondo Europeo de Desarrollo Regional
Agencia Estatal de Investigación

Overview

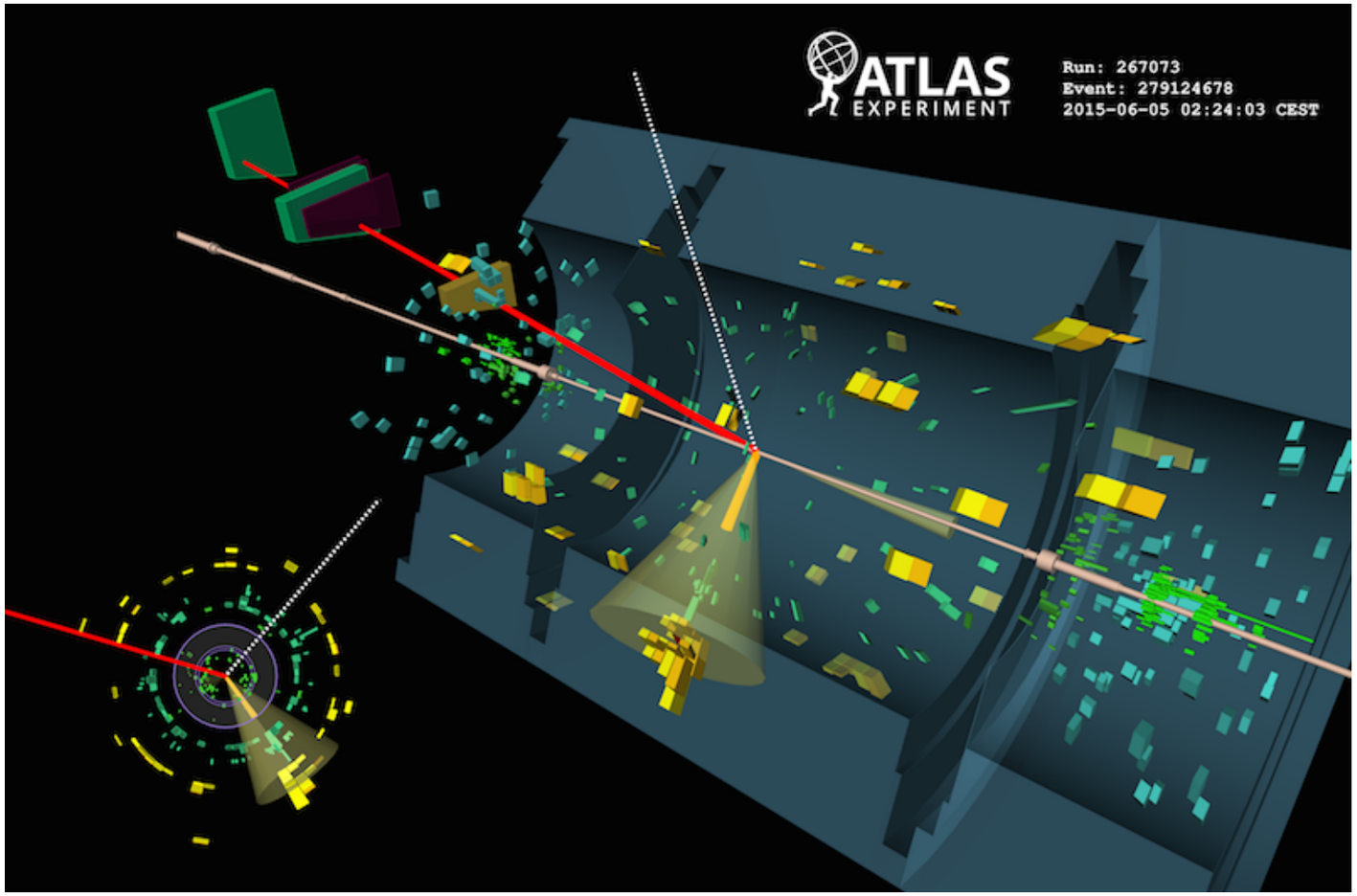

- **Quadruple differential analysis**
  - Analysis method
  - Techniques developed
  - Region definition
  - Analysis workflow
  - Results and conclusions

Mariam Chitishvili
Instituto de Fisica Corpuscular (IFIC)-CSIC/UV

Introduction and Overview

The top quark was discovered by the Tevatron experiments, CDF and D0, at Fermilab in 1995.

- Tevatron Run-II (10^{32} cm^{-2} s^{-1} @ 1.96 TeV): ~2 top pair every hour.

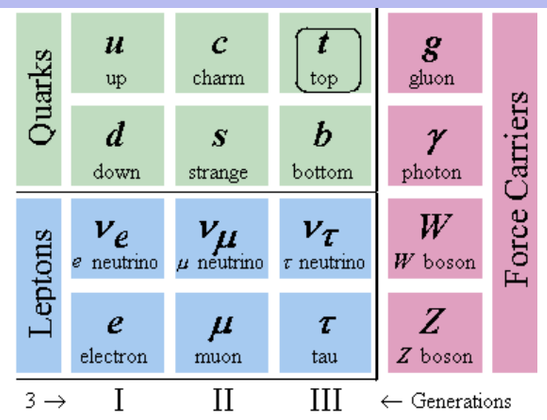

The LHC is a top quark factory:

- At low luminosity (i.e. 10^{32} cm^{-2} s^{-1} @ 7 TeV): ~60 top pair every hour.
- At design luminosity (i.e. 10^{34} cm^{-2} s^{-1} @ 14 TeV): ~8 top pair every second.

- Heaviest known elementary particle.
- Smallest cross-section of all of the SM particles.
- Short lifetime $(\tau_t \approx 5 \cdot 10^{-25} s) \Rightarrow$ top-quark decays into high pT particles before hadronizing
- Unique quark: only quark whose most of its properties can be directly measured!!!
- The top quark decays almost exclusively (>99%, i.e. $|V_{tb}| \approx 0.999$) to t → Wb (LO)
- Produced in pairs and singly at the LHC

Feynman diagrams of single top

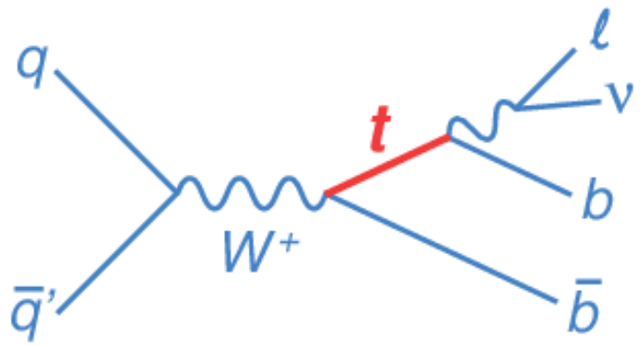

Mariam Chitishvili
Instituto de Fisica Corpuscular (IFIC)-CSIC/UV

Quadruple differential analysis method

- The top-quark decay differential distribution is determined by four angles (Eur. Phys. J. C77, 200 (2017)):

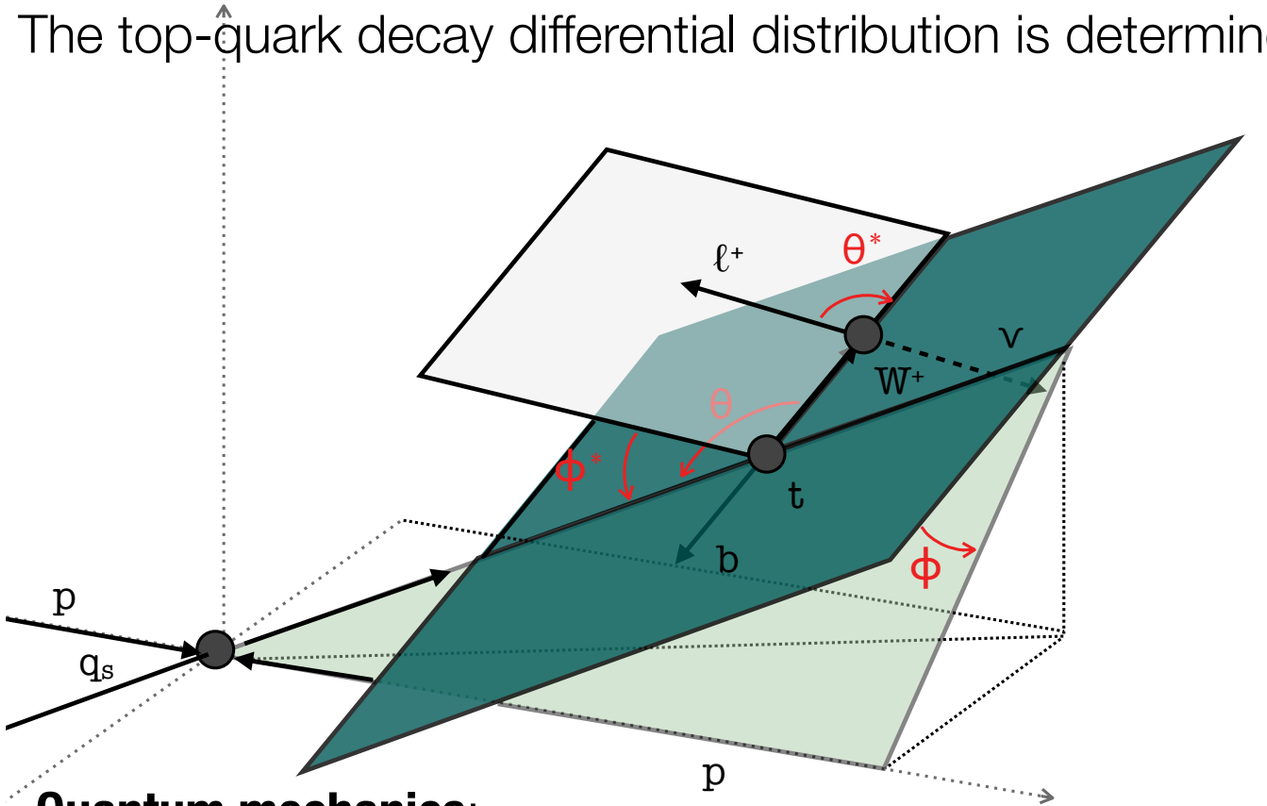

In the tWb vertex ($t \to Wb \to l\nu$):

- ϕ, θ are spherical coordinates of the W boson momentum in the top quark rest frame
- ϕ^*, θ^* spherical coordinates of the charged lepton momentum in the W boson rest frame

Quantum mechanics:

- The fully differential decay rate can be written **analytically** by applying the helicity formalism of Jacob and Wick to polarised top quarks in the t-channel production, considering the transition amplitudes (in the narrow width approximation)

$$\frac{1}{\Gamma}\frac{d\Gamma}{d\Omega d\Omega^*} \propto |A(t \to Wb) \cdot A(W \to l\nu)|^2$$

arXiv:1304.5639 [hep-ex]

- The angular dependence of the amplitude for a two-body decay is

$$A(t \to W^+ b) = \left[\frac{1}{2\pi}\right]^{\frac{1}{2}} D^{\frac{1}{2}}_{\frac{1}{2},\lambda_W-\lambda_b}{}^*(\varphi,\theta,-\varphi) A_{\lambda_W,\lambda_b}\,,$$

$$A(W^+ \to l^+\nu) = \left[\frac{3}{4\pi}\right]^{\frac{1}{2}} D^{1}_{\lambda_W,1}{}^*(\varphi^*,\theta^*,-\varphi^*) A_{\frac{1}{2},-\frac{1}{2}}\,;$$

Transition amplitudes

Wigner D-function

Mariam Chitishvili
Instituto de Fisica Corpuscular (IFIC)-CSIC/UV

Quadruple differential analysis method

The Lagrangian of the **Standard Model** (SM), includes terms that account for the particles and interactions. Despite its success, the SM is known to be incomplete.

SMEFT Approach: Systematic BSM Effects

SMEFT introduces higher-dimensional operators to capture possible effects of unknown high-energy physics. The SMEFT Lagrangian is expanded as:

$$\mathscr{L}_{\mathbf{eff}} = \mathscr{L}^{(4)}_{\mathbf{SM}} + \frac{1}{\Lambda}\sum_i c_i^{(5)} O_i^{(5)} + \frac{1}{\Lambda^2}\sum_i c_i^{(6)} O_i^{(6)} + O\left(\frac{1}{\Lambda^3}\right)$$

The analysis sensitivity requires expansion up to dimension-6 operators. These operators introduce new interactions that are not present in the SM.

The (EFT) coefficients measuring strength of these operators sensitive to the analysis, — **Wilson Coefficients**:

- c_{tw}, c_{itw} describing top quark and W boson interactions.
- c_{bw}, c_{ibw} describing bottom quark and W boson interactions.
- c_{Qq} involving four-quark interactions.
- $c_{\phi tb}$ involving top, bottom quark and Higgs field interactions
- $c_{\phi q}$ involving top quark and Higgs field

Analysis techniques

Quadruple differential decay rate depending on the four angles covers full phase space and can be expressed with orthonormal function (let's call it M) and 24 coefficients. arXiv:1304.5639 [hep-ex]

Because of the orthonormality of the M functions, the different coefficients can be determined by projecting the differential distribution in a manner similar to Fourier analysis.

Finite series of orthonormal M-functions

$$\frac{1}{\Gamma}\frac{d\Gamma}{d\Omega d\Omega^*} = \sum_{j_1 j_2 m' m} c^{j_1 j_2}_{m' m} M^{j_1 j_2}_{m' m}(\phi, \theta, \phi^*, \theta^*)^*$$

24 angular coefficients to be determined

$$c^{j_1 j_2}_{m' m} = \int d\Omega\, d\Omega^*\; g(\phi, \theta, \phi^*, \theta^*)\, M^{j_1 j_2}_{m' m}(\phi, \theta, \phi^*, \theta^*)^*$$

Mariam Chitishvili
Instituto de Fisica Corpuscular (IFIC)-CSIC/UV

Analysis techniques

$$\frac{1}{\Gamma}\frac{d\Gamma}{d\Omega d\Omega^*} = \frac{3}{64\pi^2}\frac{1}{\mathcal{N}}\left\{\left[|a_{1\,\frac{1}{2}}|^2(1+\lambda\cos\theta^*)^2 + 2|a_{0\,-\frac{1}{2}}|^2\sin^2\theta^*\right]\left(1+\vec{P}\cdot\vec{u}_L\right)\right.$$
$$+\left[2|a_{0\,\frac{1}{2}}|^2\sin^2\theta^* + |a_{-1\,-\frac{1}{2}}|^2(1-\lambda\cos\theta^*)^2\right]\left(1-\vec{P}\cdot\vec{u}_L\right)$$
$$+\lambda 2\sqrt{2}\left[\mathrm{Re}(a_{0\,\frac{1}{2}}a^*_{1\,\frac{1}{2}}e^{-i\phi^*})(1+\lambda\cos\theta^*)\right.$$
$$\left.+\mathrm{Re}(a_{-1\,-\frac{1}{2}}a^*_{0\,-\frac{1}{2}}e^{-i\phi^*})(1-\lambda\cos\theta^*)\right]\sin\theta^*\vec{P}\cdot\vec{u}_T$$
$$+\lambda 2\sqrt{2}\left[\mathrm{Im}(a_{0\,\frac{1}{2}}a^*_{1\,\frac{1}{2}}e^{-i\phi^*})(1+\lambda\cos\theta^*)\right.$$
$$\left.\left.+\ \mathrm{Im}(a_{-1\,-\frac{1}{2}}a^*_{0\,-\frac{1}{2}}e^{-i\phi^*})(1-\lambda\cos\theta^*)\right]\sin\theta^*\vec{P}\cdot\vec{u}_N\right\}.$$

$$\frac{1}{\Gamma}\frac{d\Gamma}{d\Omega d\Omega^*} = \sum_{j_1 j_2 m' m} c^{j_1 j_2}_{m' m} M^{j_1 j_2}_{m' m}(\phi,\theta,\phi^*,\theta^*)^*$$

$$c^{00}_{00} = \frac{1}{4\pi},$$
$$c^{10}_{00} = \frac{1}{4\sqrt{3}\pi}P_z\left[|a_{1\,\frac{1}{2}}|^2 - |a_{0\,\frac{1}{2}}|^2 + |a_{0\,-\frac{1}{2}}|^2 - |a_{-1\,-\frac{1}{2}}|^2\right]/\mathcal{N},$$
$$c^{10}_{10} = -(c^{10}_{-10})^* = -\frac{1}{4\sqrt{6}\pi}(P_x+iP_y)\left[|a_{1\,\frac{1}{2}}|^2 - |a_{0\,\frac{1}{2}}|^2 + |a_{0\,-\frac{1}{2}}|^2 - |a_{-1\,-\frac{1}{2}}|^2\right]/\mathcal{N},$$
$$c^{01}_{00} = \lambda\frac{\sqrt{3}}{8\pi}\left[|a_{1\,\frac{1}{2}}|^2 - |a_{-1\,-\frac{1}{2}}|^2\right]/\mathcal{N},$$
$$c^{11}_{00} = \lambda\frac{1}{8\pi}P_z\left[|a_{1\,\frac{1}{2}}|^2 + |a_{-1\,-\frac{1}{2}}|^2\right]/\mathcal{N},$$
$$c^{11}_{10} = -(c^{11}_{-10})^* = -\lambda\frac{1}{8\sqrt{2}\pi}(P_x+iP_y)\left[|a_{1\,\frac{1}{2}}|^2 + |a_{-1\,-\frac{1}{2}}|^2\right]/\mathcal{N},$$
$$c^{11}_{01} = (c^{11}_{0-1})^* = \lambda\frac{1}{4\sqrt{2}\pi}P_z\left[a_{0\,\frac{1}{2}}\,a^*_{1\,\frac{1}{2}} + a_{-1\,-\frac{1}{2}}\,a^*_{0\,-\frac{1}{2}}\right]/\mathcal{N},$$
$$c^{11}_{11} = -(c^{11}_{-1-1})^* = -\lambda\frac{1}{8\pi}(P_x+iP_y)\left[a_{0\,\frac{1}{2}}\,a^*_{1\,\frac{1}{2}} + a_{-1\,-\frac{1}{2}}\,a^*_{0\,-\frac{1}{2}}\right]/\mathcal{N},$$
$$c^{11}_{1-1} = -(c^{11}_{-11})^* = -\lambda\frac{1}{8\pi}(P_x+iP_y)\left[a_{1\,\frac{1}{2}}\,a^*_{0\,\frac{1}{2}} + a_{0\,-\frac{1}{2}}a^*_{-1\,-\frac{1}{2}}\right]/\mathcal{N},$$
$$c^{02}_{00} = \frac{1}{8\sqrt{5}\pi}\left[|a_{1\,\frac{1}{2}}|^2 - 2|a_{0\,\frac{1}{2}}|^2 - 2|a_{0\,-\frac{1}{2}}|^2 + |a_{-1\,-\frac{1}{2}}|^2\right]/\mathcal{N},$$
$$c^{12}_{00} = \frac{1}{8\sqrt{15}\pi}P_z\left[|a_{1\,\frac{1}{2}}|^2 + 2|a_{0\,\frac{1}{2}}|^2 - 2|a_{0\,-\frac{1}{2}}|^2 - |a_{-1\,-\frac{1}{2}}|^2\right]/\mathcal{N},$$
$$c^{12}_{10} = -(c^{12}_{-10})^* = -\frac{1}{8\sqrt{30}\pi}(P_x+iP_y)\left[|a_{1\,\frac{1}{2}}|^2 + 2|a_{0\,\frac{1}{2}}|^2 - 2|a_{0\,-\frac{1}{2}}|^2 - |a_{-1\,-\frac{1}{2}}|^2\right]/\mathcal{N},$$
$$c^{12}_{01} = (c^{12}_{0-1})^* = \frac{1}{4\sqrt{10}\pi}P_z\left[a_{0\,\frac{1}{2}}\,a^*_{1\,\frac{1}{2}} - a_{-1\,-\frac{1}{2}}\,a^*_{0\,-\frac{1}{2}}\right]/\mathcal{N},$$
$$c^{12}_{11} = -(c^{12}_{-1-1})^* = -\frac{1}{8\sqrt{5}\pi}(P_x+iP_y)\left[a_{0\,\frac{1}{2}}\,a^*_{1\,\frac{1}{2}} - a_{-1\,-\frac{1}{2}}\,a^*_{0\,-\frac{1}{2}}\right]/\mathcal{N},$$
$$c^{12}_{1-1} = -(c^{12}_{-11})^* = -\frac{1}{8\sqrt{5}\pi}(P_x+iP_y)\left[a_{1\,\frac{1}{2}}\,a^*_{0\,\frac{1}{2}} - a_{0\,-\frac{1}{2}}\,a^*_{-1\,-\frac{1}{2}}\right]/\mathcal{N}.$$

Mariam Chitishvili
Instituto de Fisica Corpuscular (IFIC)-CSIC/UV

Analysis techniques

- The analysis uses **morphing technique** modeling the response of M-function coefficients to variations in Wilson coefficients. It employs a set of orthonormal polynomials of 4th order to capture the dependence of these coefficients on the Wilson parameters for different processes.

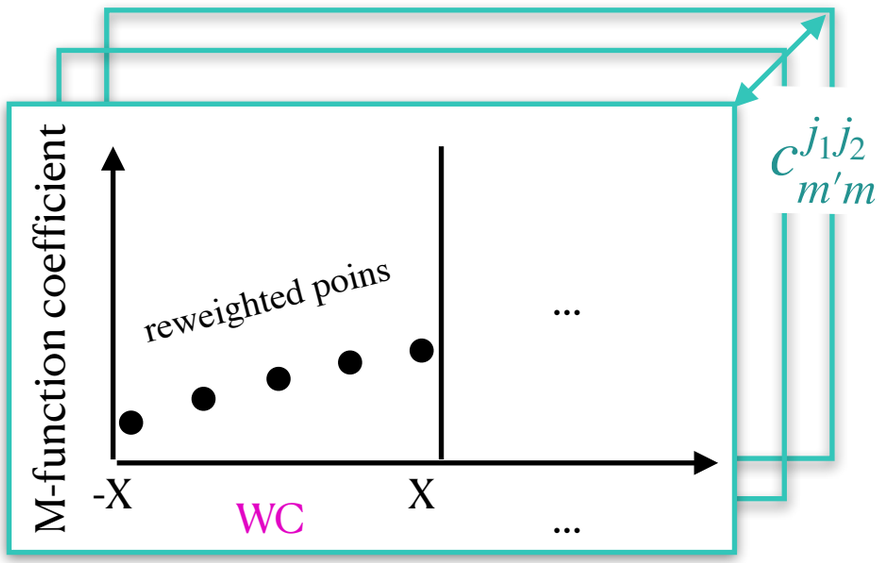

- The plot show morphs of the expected event yield in the signal region varies with individual Wilson coefficients, providing a direct view of the impact of each operator.
- They are used to validate the morphing setup and identify which coefficients drive the largest deviations, helping to optimize the sensitivity of the fit across different phase space regions.

$$\sim \sum c^{j_1 j_2}_{m'm}$$

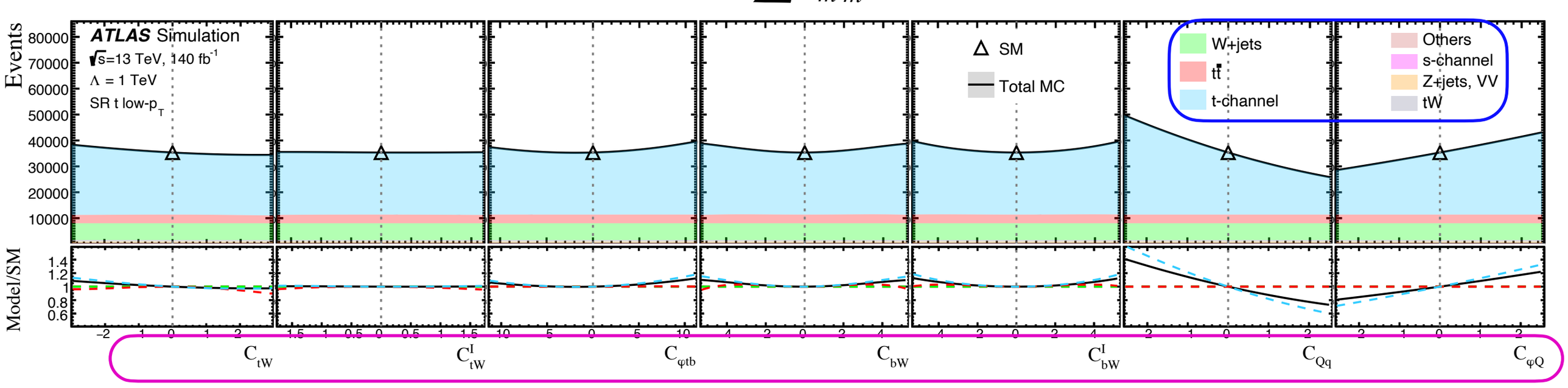

Region definition

- The analysis is divided into a signal region (SR), targeting t-channel single top-quark production, and two control regions enriched in $t\bar{t}$ and W+jets events.
- SR is further split based on the charge of the reconstructed top quark (top vs. anti-top) and its transverse momentum, separating events into low-pT and high-pT of the top quark categories using a threshold of pT =80GeV.

  - **In total 4X23 M-function coefficients are modeled for the signal channels**

The common event selection

Preselection region	Signal region	$t\bar{t}$ control region	W+jets control region
=1 charged tight lepton ($p_{\mathrm{T}} > 30$ GeV and $\lvert\eta\rvert < 2.5$) Veto secondary low-p_{T} charged loose leptons ($p_{\mathrm{T}} > 10$ GeV and $\lvert\eta\rvert < 2.5$) =2 jets ($p_{\mathrm{T}} > 30$ GeV and $\lvert\eta\rvert < 4.5$; $p_{\mathrm{T}} > 35$ GeV within $2.7 < \lvert\eta\rvert < 3.5$) $E_{\mathrm{T}}^{\mathrm{miss}} > 35$ GeV $m_{\mathrm{T}}(\ell E_{\mathrm{T}}^{\mathrm{miss}}) > 60$ GeV $p_{\mathrm{T}}(\ell) > 50\left(1 - \frac{\pi - \lvert\Delta\phi(j_1,\ell)\rvert}{\pi - 1}\right)$ GeV			
=1 b-jet ($\lvert\eta\rvert < 2.5$; 60%WP)		=2 b-jet ($\lvert\eta\rvert < 2.5$; 60%WP)	=1 b-jet ($\lvert\eta\rvert < 2.5$; 60%WP)
	$m_{\ell b} < 153$ GeV $m_{\ell E_{\mathrm{T}}^{\mathrm{miss}} b} \in [120.6, 234.6]$ GeV trapez. requirement $m_{j\ell E_{\mathrm{T}}^{\mathrm{miss}} b} > 320$ GeV $H_{\mathrm{T}} > 190$ GeV		$m_{\ell b} > 153$ GeV $m_{\ell E_{\mathrm{T}}^{\mathrm{miss}} b} \notin [120.6, 234.6]$ GeV veto trapez. requirement $m_{j\ell E_{\mathrm{T}}^{\mathrm{miss}} b} < 320$ GeV $H_{\mathrm{T}} < 190$ GeV
	$\mathscr{L}_K > -36$		

Mariam Chitishvili
Instituto de Fisica Corpuscular (IFIC)-CSIC/UV

Analysis workflow

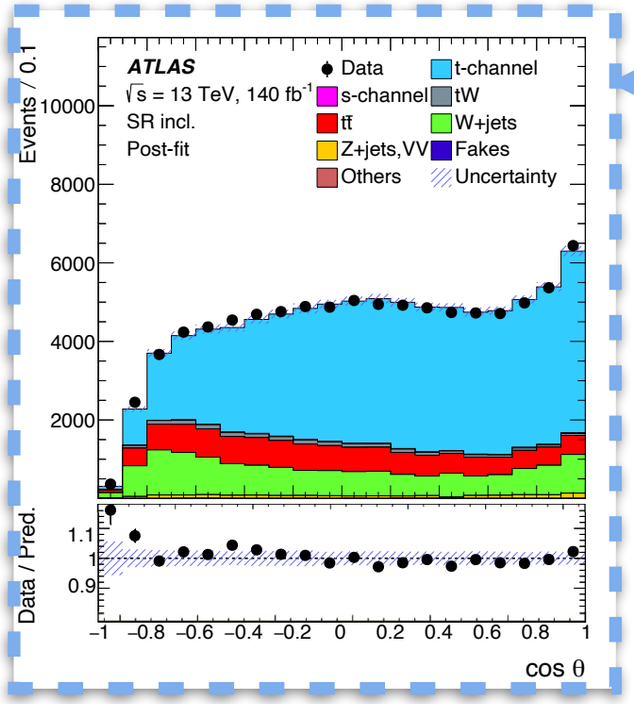

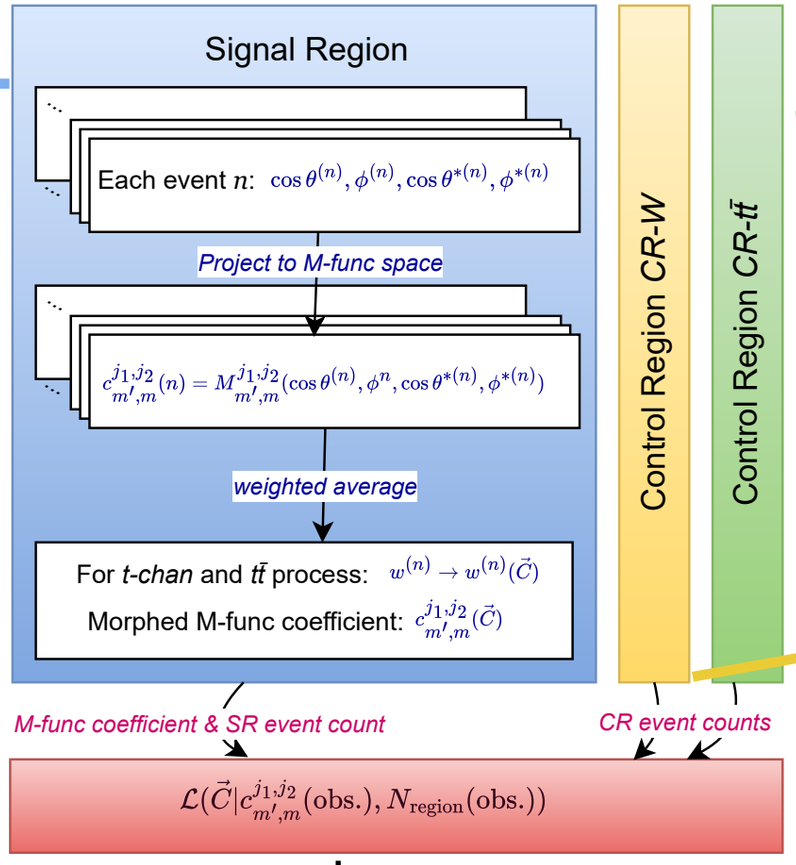

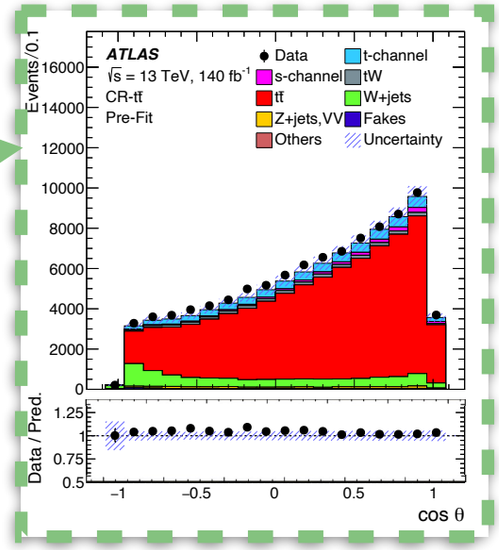

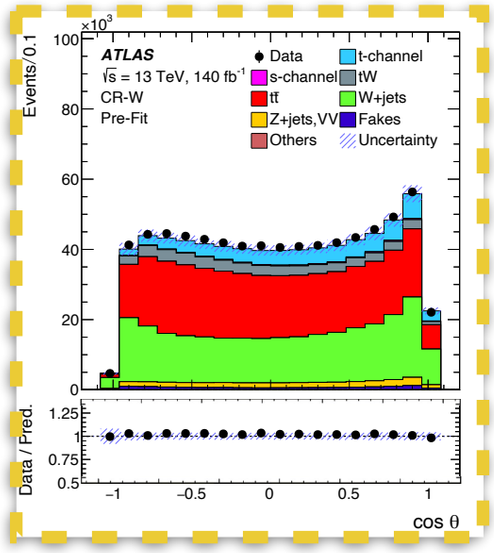

The foundation of the fitting process is a likelihood function, which is then maximised to identify parameter values that best align with the observed data.

$$\ln L(\vec{C},\vec{S}) = -\frac{1}{2}\sum_{(s)}\left[\left(\vec{c}^{(s)} - \vec{c}^{(s),\text{model}}(\vec{C},\vec{S})\right)^{T}\mathbb{C}^{(s)-1}\left(\vec{c}^{(s)} - \vec{c}^{(s),\text{model}}(\vec{C},\vec{S})\right) + \sum_{j\in\{\text{SR,CR1,CR2}\}}\frac{\left(N^{(s,j),\text{model}}(\vec{C},\vec{S}) - N^{(s,j)}\right)^{2}}{N^{(s,j)}}\right]$$

Vector of EFT parameters

Vector of scale factors

Mariam Chitishvili
Instituto de Fisica Corpuscular (IFIC)-CSIC/UV

The results

The analysis performs a simultaneous fit **considering all four angles for the first time**, allowing us to explore the full phase space of the top quark decay. This comprehensive approach enhances the sensitivity to the Wilson coefficients and provides a more precise and complete understanding of the underlying physics.

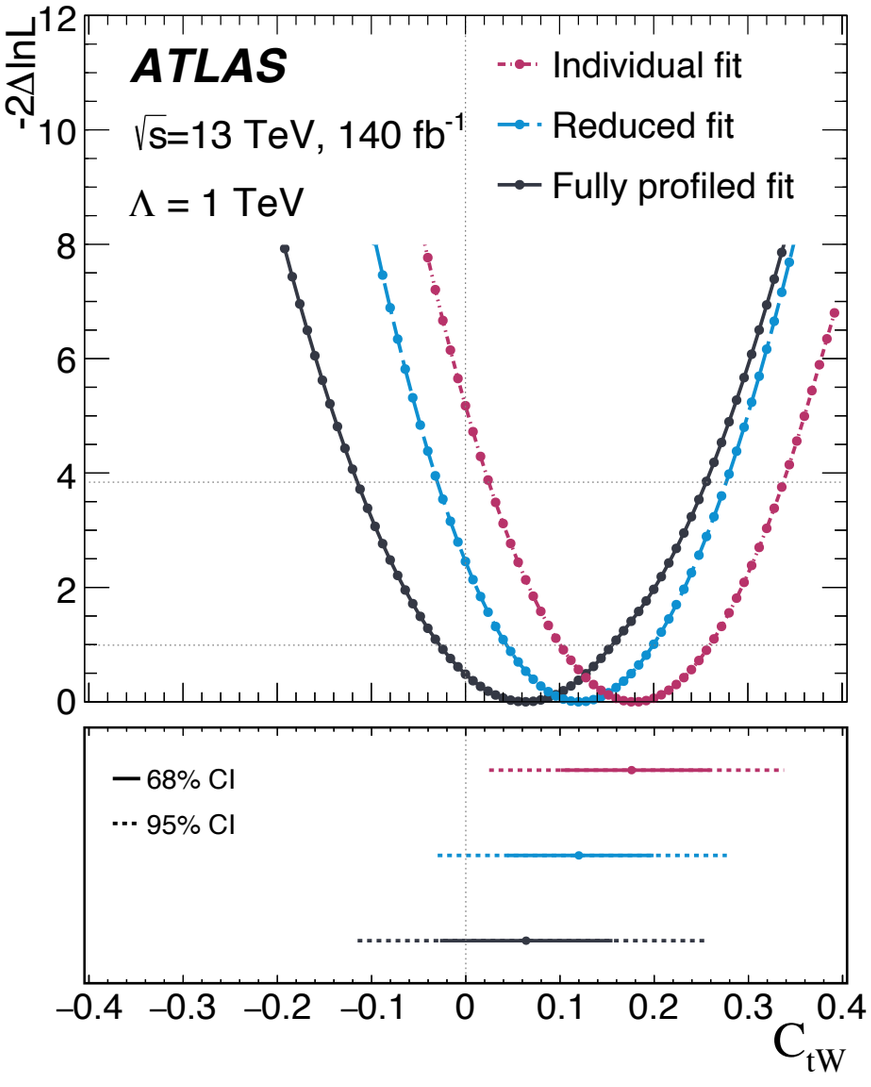

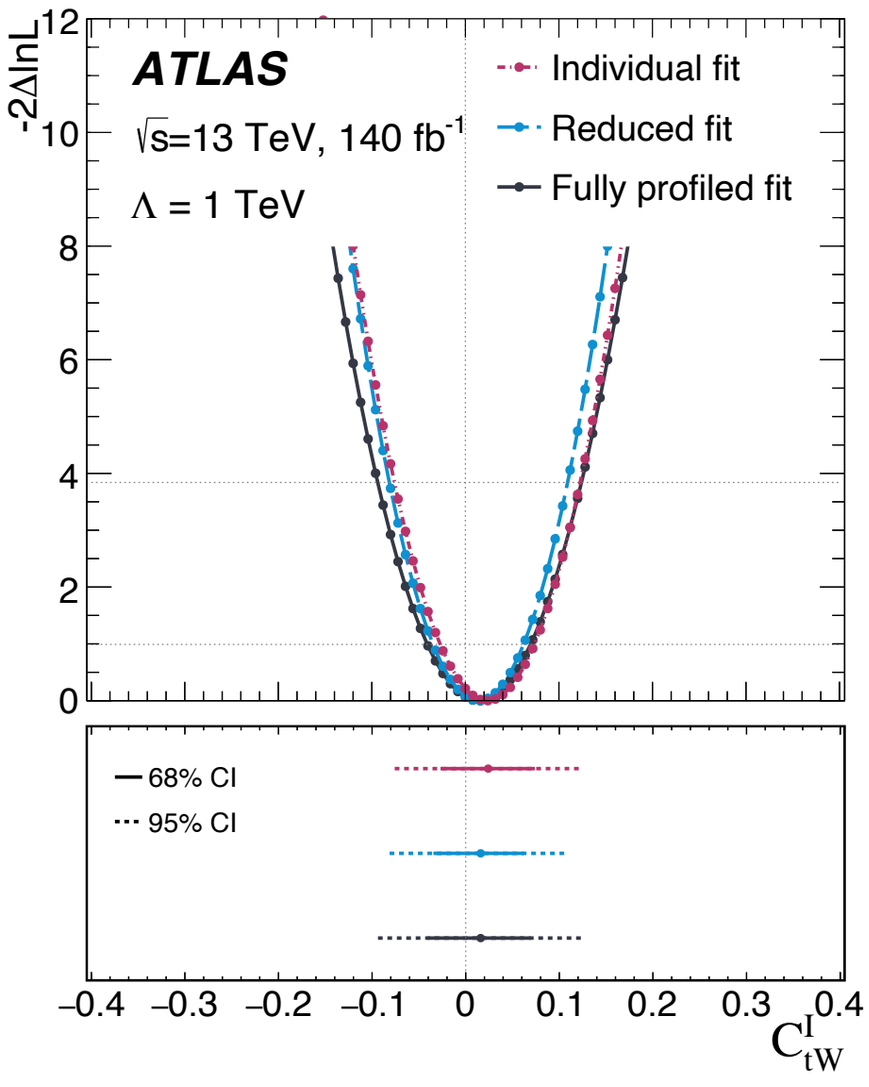

Individual:
One Wilson coefficient is varied at a time; all others are fixed to zero.

Reduced fit:
Only linear (interference) terms in the Wilson coefficients are fitted, others are fixed. Sensitive to interference effects and avoids bias from O(1/Λ4) terms.

Fully profiled:
All Wilson coefficients are floated simultaneously. each POI is scanned while profiling the other six POIs. Captures correlations and degeneracies;

The results

- In a 1D likelihood scan, the value of a single parameter of interest (POI) is varied while profiling all other parameters to maximize the likelihood, allowing us to quantify how well different values of that POI are supported by the data through the test statistic $-2\ln\dfrac{\mathscr{L}(C_i,\hat{C}_j)}{\mathscr{L}(\hat{C})}$

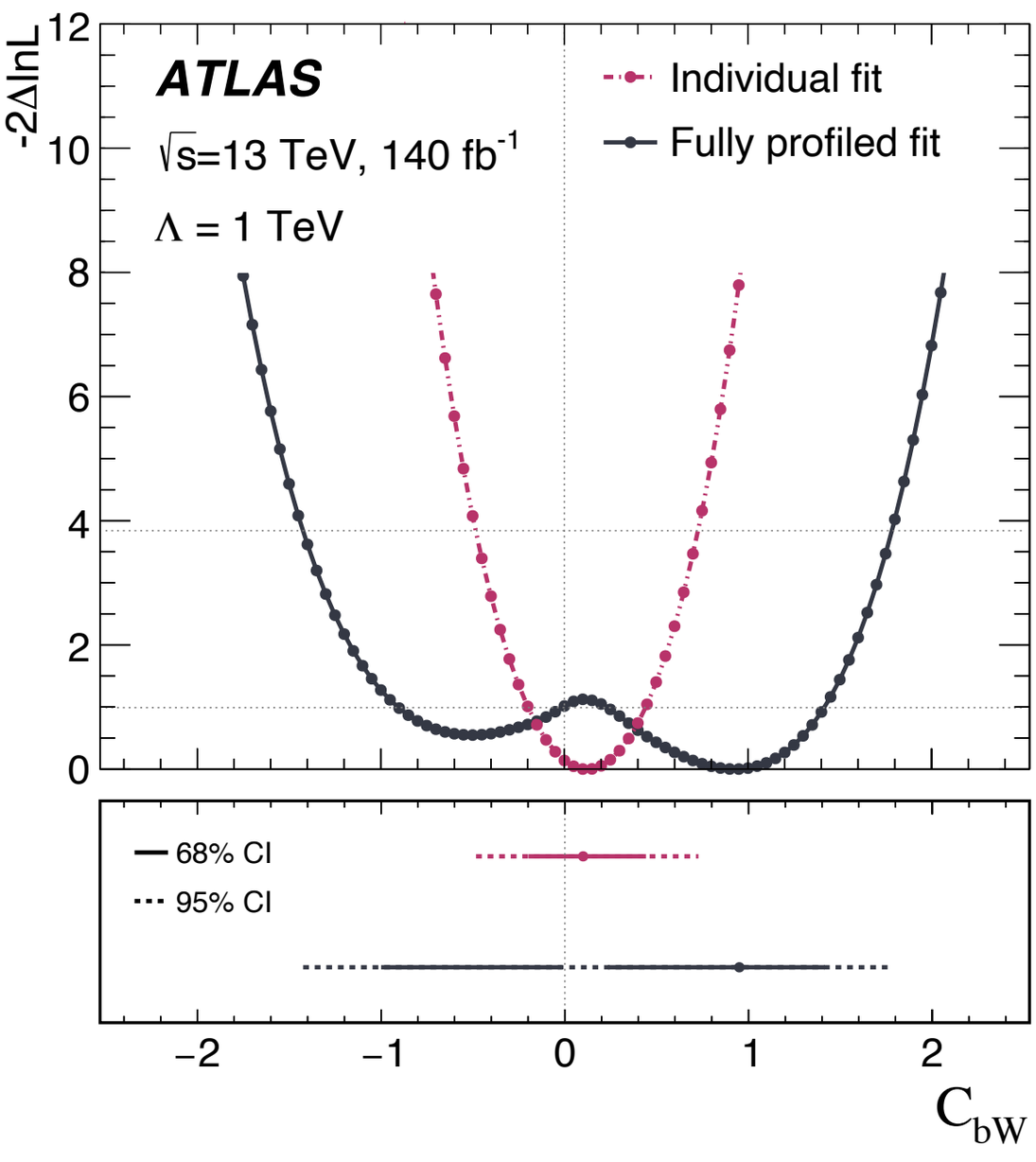

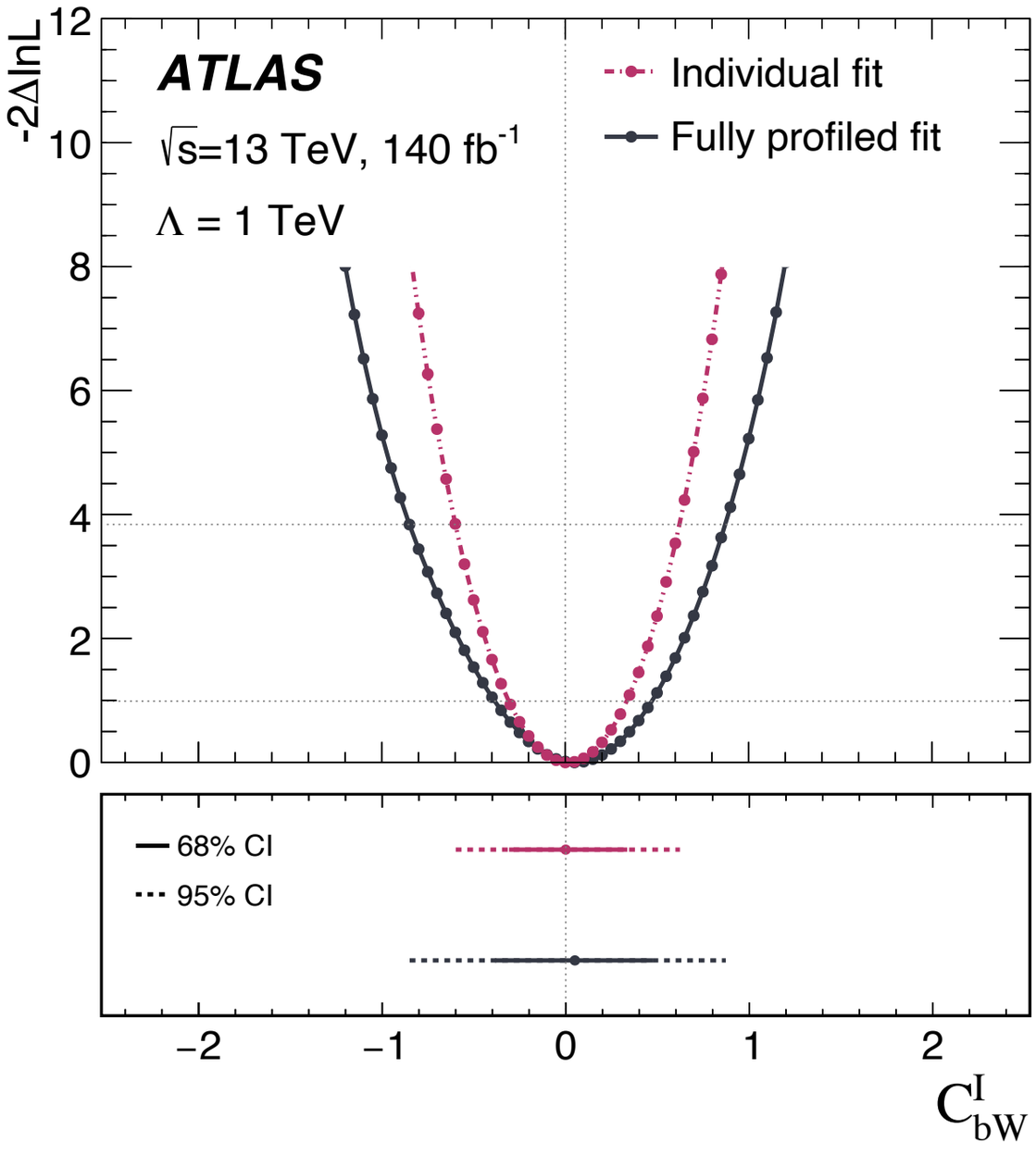

Mariam Chitishvili
Instituto de Fisica Corpuscular (IFIC)-CSIC/UV

The results

Double-minimum likelihood shapes in data

In two cases, the 1D likelihood scan for a POI shows a double-minimum structure when using real data, but not with the Asimov dataset. This means the likelihood has two separated regions in parameter space that are both locally preferred by the data.

- This can happen when the data "crosses" the expected SM prediction in a way that the fit finds two disjoint minima, each giving similarly good agreement.
- It often reflects non-Gaussian behavior or interference effects, especially in the presence of complex EFT phases or subtle mismodeling.
- It may also suggest the fit is not locating the true global minimum due to a complicated landscape.

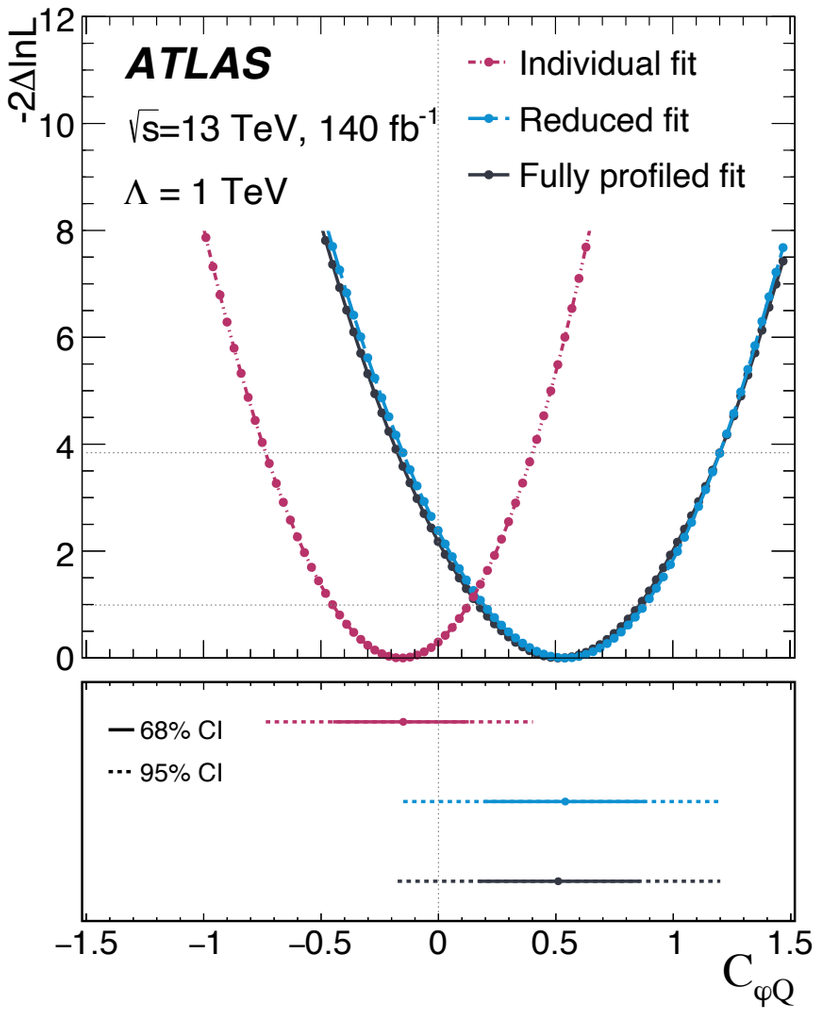

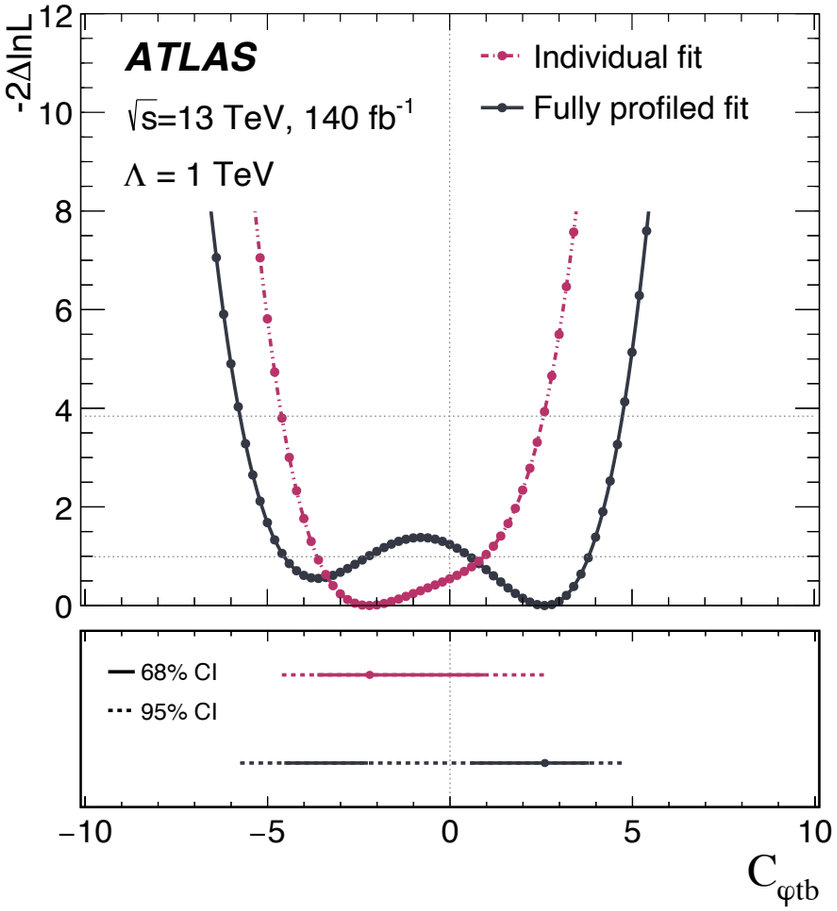

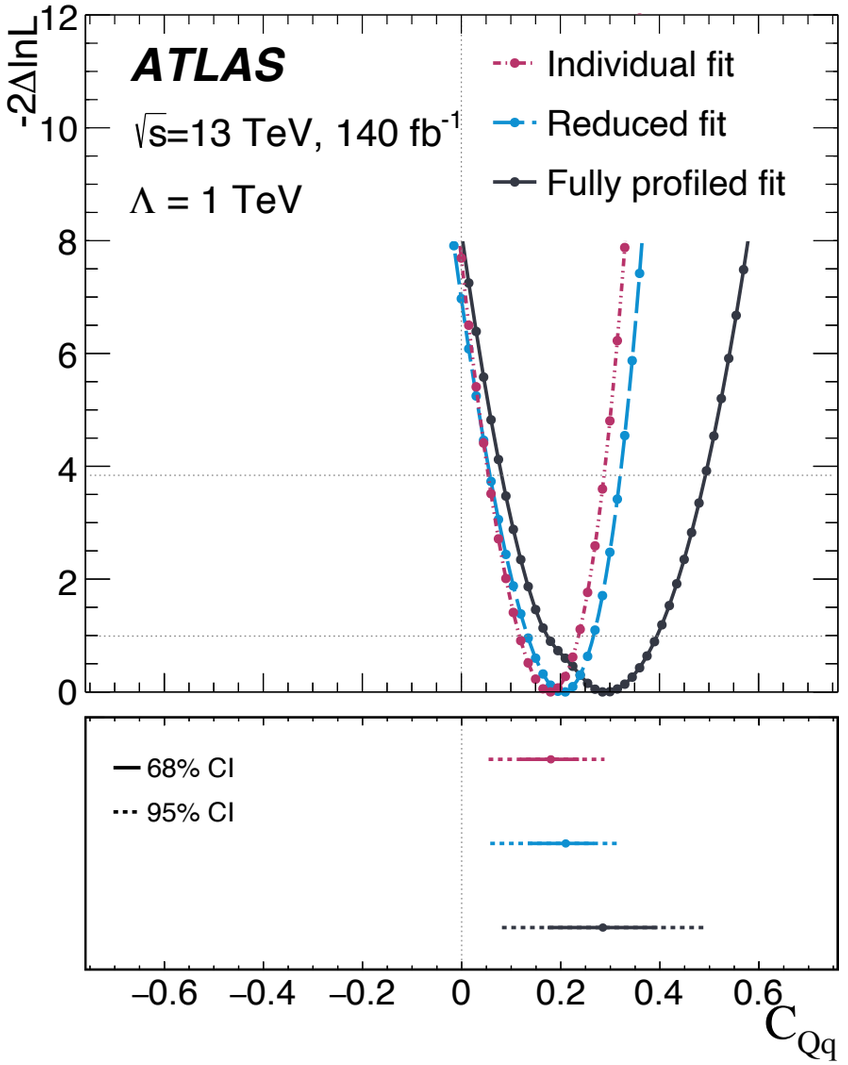

Fit diagnostics

- The systematic uncertainty is taken into account by computing a covariance matrix for the systematic uncertainty sources:

$$\mathbb{C}^{\text{syst.}} = \sum_{\text{syst. sources}} \Delta\vec{\nu} \otimes \Delta\vec{\nu}^{T}$$

Where $\Delta\vec{\nu}$ is a vector of the expected 1sigma uncertainty.

Source of uncertainty	C_{tW}	C_{tW}^{I}	$C_{\varphi tb}$	C_{bW}	C_{bW}^{I}	C_{Qq}	$C_{\varphi Q}$
Jet energy scale	−0.03, +0.03	−0.01, +0.01	−0.6, +0.4	−0.3, +0.3	−0.3, +0.3	−0.02, +0.05	−0.10, +0.09
Pile-up	−0.01, –	–	−0.1, +0.2	–, +0.1	−0.1, –	–, +0.01	−0.08, +0.06
b-tagging	−0.02, +0.03	−0.01, +0.01	−0.6, +0.6	−0.1, +0.2	−0.1, +0.1	−0.02, +0.02	−0.13, +0.13
Jet energy resolution	−0.02, +0.02	−0.01, +0.01	−0.8, +0.7	−0.1, +0.1	−0.1, +0.1	−0.02, +0.03	−0.08, +0.09
PDF	−0.02, +0.02	−0.01, +0.01	−0.7, +0.6	−0.1, +0.1	−0.1, +0.1	−0.03, +0.04	−0.08, +0.09
Muon	−0.03, +0.02	–	−0.4, +0.3	−0.1, +0.1	−0.1, +0.1	−0.01, +0.03	−0.07, +0.06
$E_{\text{T}}^{\text{miss}}$	−0.02, +0.02	–	−0.5, +0.4	−0.1, +0.1	−0.2, +0.2	−0.01, +0.02	−0.06, +0.05
e/γ	−0.01, +0.01	–	−0.2, +0.1	−0.1, +0.1	−0.1, +0.1	–, +0.01	−0.06, +0.07
Jet vertex tagging	−0.01, +0.01	–	−0.1, +0.2	–, +0.1	–	−0.02, +0.03	−0.17, +0.18
Lumi. & cross-section	−0.01, –	–	−0.1, +0.1	−0.1, +0.1	−0.1, +0.1	−0.01, –	−0.07, +0.07
τ_{had} energy scale	–	–	–	–	–	–	–
Non-prompt leptons	−0.01, –	–	–, +0.2	–, +0.1	−0.1, +0.1	−0.01, –	−0.01, +0.01
t-channel modelling	−0.01, +0.01	–	−0.3, +0.1	–	–	−0.04, +0.04	−0.15, +0.15
$t\bar{t}$ modelling	−0.03, +0.02	−0.01, –	−0.5, +0.4	−0.1, +0.1	−0.1, +0.1	−0.01, +0.03	−0.04, +0.08
W+ jets modelling	−0.01, +0.02	−0.01, +0.01	−0.8, +0.6	−0.1, +0.1	–, +0.1	−0.01, +0.02	−0.06, +0.08
MC sample sizes	−0.03, +0.03	−0.03, +0.03	−0.9, +0.8	−0.2, +0.2	−0.2, +0.2	−0.03, +0.05	−0.14, +0.14
Data sample size	−0.06, +0.05	−0.04, +0.04	−3.1, +1.7	−0.5, +0.7	−0.5, +0.5	−0.05, +0.08	−0.13, +0.15
Total	−0.10, +0.09	−0.06, +0.06	−3.9, +2.6	−0.8, +0.9	−0.7, +0.7	−0.09, +0.14	−0.41, +0.43

The total systematic uncertainty is comparable to the statistical uncertainty of the data except for $C_{\phi Q}$, but no individual source of systematic uncertainty significantly outweighs the total statistical uncertainty

Mariam Chitishvili
Instituto de Fisica Corpuscular (IFIC)-CSIC/UV

Fit diagnostics

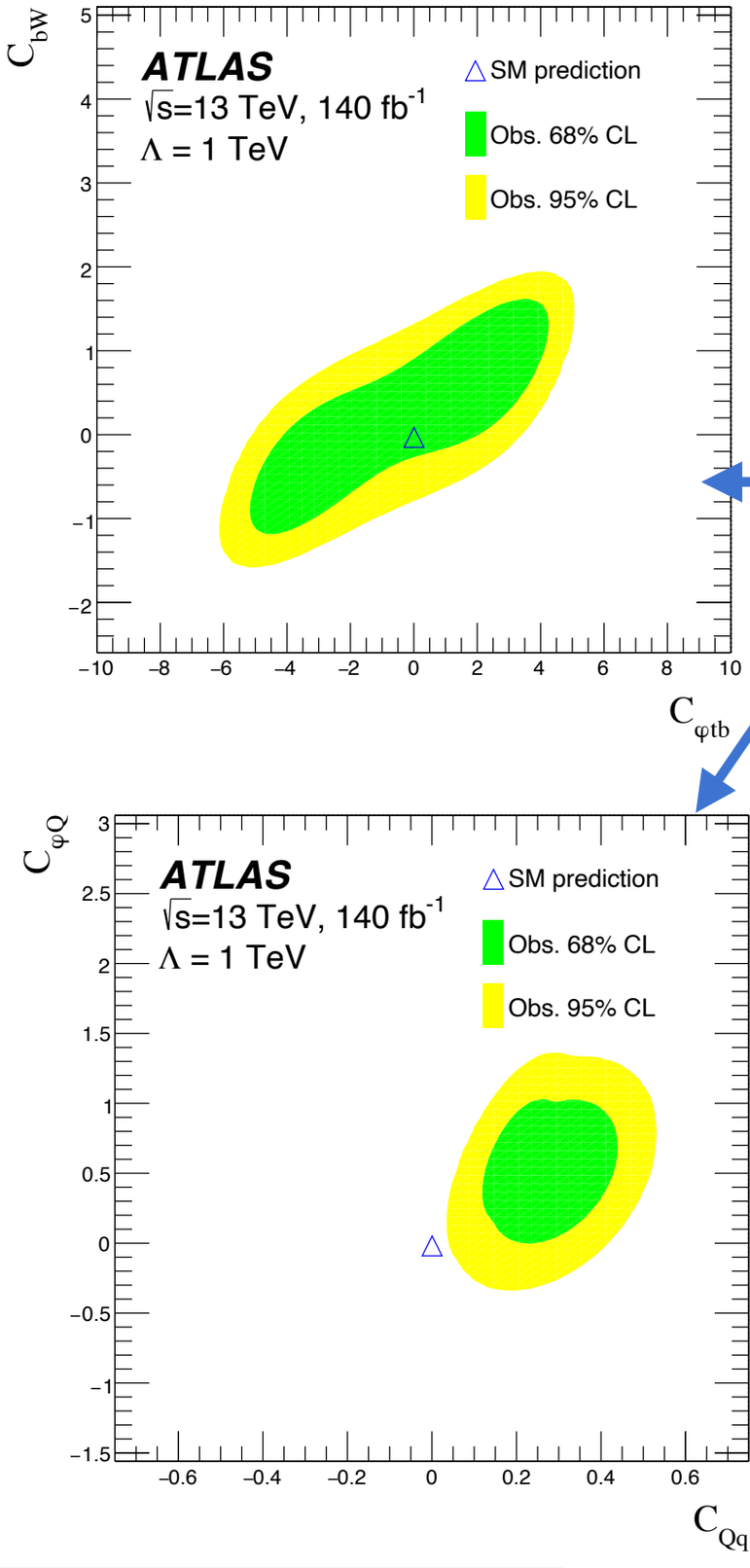

- 2D likelihood scans properly visualize the shape of the parameter space and reveal complex structures of parameter dependencies.

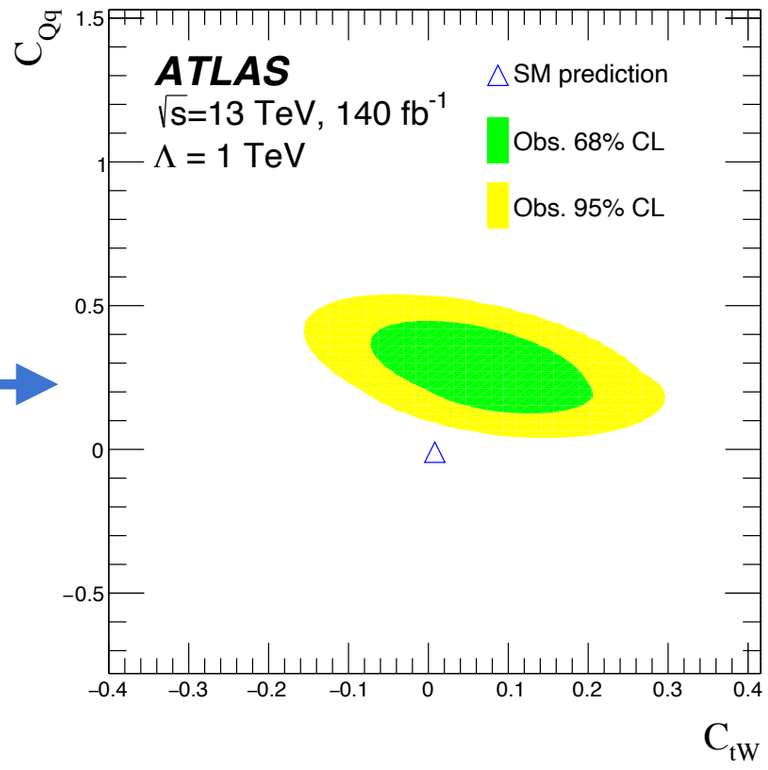

- **Covariance matrix** for the reduced fit, which is a linear sum of statistical covariance from data and statistical covariance from MC

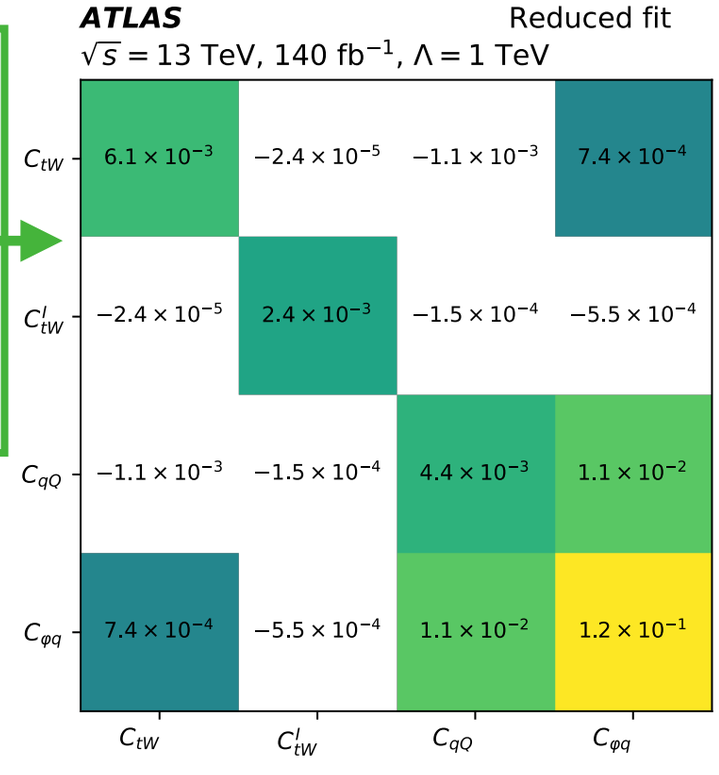

Mariam Chitishvili
Instituto de Fisica Corpuscular (IFIC)-CSIC/UV

The results

- We show 95% CL limits on Wilson coefficients from a quadruple-differential analysis of single top events at $\sqrt{s} = 13$ TeV with 140 fb^{-1} of data.

- The results show improvement in current limits for C_{tw}, C_{itw}, highlighting the strong sensitivity of angular observables to interference and CP-violating effects.

Wilson coefficient [TeV^{-2}]	**Fully profiled fit** 68% CL interval	95% CL interval	**Individual fit** 68% CL interval	95% CL interval
C_{tW}/Λ^2	$[-0.03, +0.17]$	$[-0.12, +0.26]$	$[+0.10, +0.26]$	$[+0.02, +0.34]$
C_{tW}^I/Λ^2	$[-0.04, +0.07]$	$[-0.10, +0.13]$	$[-0.03, +0.07]$	$[-0.08, +0.12]$
$C_{\varphi tb}/\Lambda^2$	$[-4.6, -2.3] \cup [+0.5, +3.8]$	$[-5.8, +4.8]$	$[-3.6, +1.0]$	$[-4.6, +2.6]$
C_{bW}/Λ^2	$[-1.0, 0.0] \cup [+0.2, +1.4]$	$[-1.4, +1.8]$	$[-0.2, +0.4]$	$[-0.5, +0.7]$
C_{bW}^I/Λ^2	$[-0.4, +0.5]$	$[-0.9, +0.9]$	$[-0.3, +0.3]$	$[-0.6, +0.6]$
C_{Qq}/Λ^2	$[+0.17, +0.37]$	$[+0.08, +0.50]$	$[+0.12, +0.24]$	$[+0.05, +0.29]$
$C_{\varphi Q}/\Lambda^2$	$[+0.17, +0.86]$	$[-0.19, +1.2]$	$[-0.45, +0.13]$	$[-0.75, +0.41]$

Confidence regions shown for 2-3-4 fold analyses:

- **Two angles** (blue/orange) — ATLAS 7 TeV, 4.6 fb [ATLAS, Phys. Rev. Lett. 114 (2015) 142001].
- **Three angles** (green/yellow) — ATLAS 8 TeV, 20.2 fb [ATLAS, Eur. Phys. J. C 77 (2017) 264].
- All **four angles** (pink/purple) — the current, 13 TeV result [arXiv:2510.23372]

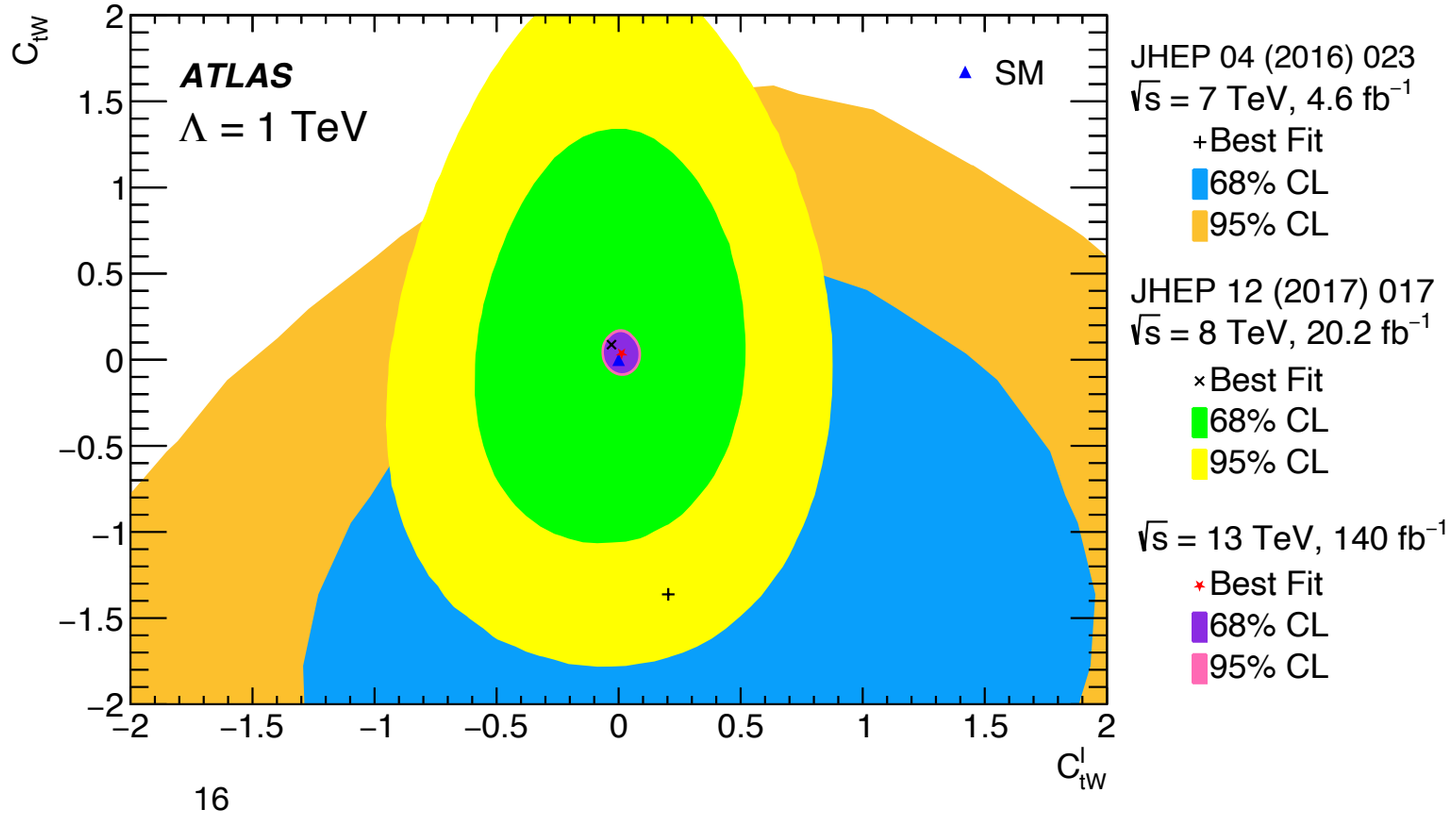

Mariam Chitishvili
Instituto de Fisica Corpuscular (IFIC)-CSIC/UV